THE JOURNAL OF BIOLOGICAL CHEMISTRY VOL. 281, NO. 45, pp. 33849–33859, November 10, 2006

Comparison of Lipoteichoic Acid from Different Serotypes of *Streptococcus pneumoniae*[*]

Received for publication, March 22, 2006, and in revised form, August 29, 2006 Published, JBC Papers in Press, August 29, 2006, DOI 10.1074/jbc.M602676200

Christian Draing[‡1], Markus Pfitzenmaier[§1], Sebastiana Zummo[¶], Giuseppe Mancuso[¶], Armin Geyer[§], Thomas Hartung[‡‖], and Sonja von Aulock[‡2]

From the Department of [‡]Biochemical Pharmacology, University of Konstanz, P. O. Box M668, 78457 Konstanz, Germany, the [§]Department of Organic Chemistry, University of Marburg, 35043 Marburg, Germany, the Department of [¶]Pathology and Experimental Microbiology, University of Messina, 98125 Messina, Italy, and the [‖]European Centre for the Validation of Alternative Methods, Joint Research Centre, 21020 Ispra, Italy

Pneumococcal lipoteichoic acid (LTA) is known to have a completely different chemical structure compared with that of *Staphylococcus aureus*: the polyglycerophosphate in the backbone is replaced in the pneumococcal LTA by a pentamer repeating unit consisting of one ribitol and a tetrasaccharide carrying the unusual substituents phosphocholine and *N*-acetyl-D-galactosamine. Neither D-alanine nor *N*-acetyl-D-glucosamine, which play central roles in the biological activity of the staphylococcal LTA, has been reported. The extraction using butanol is more gentle compared with the previously reported chloroform-methanol extraction and results in a higher yield of LTA. We characterized the LTA of two different strains of *Streptococcus pneumoniae*: R6 (serotype 2) and Fp23 (serotype 4). NMR analysis confirmed the structure of LTA from R6 but showed that its ribitol carries an *N*-acetyl-D-galactosamine substituent. The NMR data for the LTA from Fp23 indicate that this LTA additionally contains ribitol-bound D-alanine. Dose-response curves of the two pneumococcal LTAs in human whole blood revealed that LTA from Fp23 was significantly more potent than LTA from R6 with regard to the induction of all cytokines measured (tumor necrosis factor, interleukin-1 (IL-1), IL-8, IL-10, granulocyte colony-stimulating factor, and interferon γ). However, other characteristics, such as lack of inhibition by endotoxin-specific LAL-F, Toll-like receptor 2 and not 4 dependence, and lack of stimulation of neutrophilic granulocytes, were shared by both LTAs. This is the first report of a difference in the structure of LTA between two pneumococcal serotypes resulting in different immunostimulatory potencies.

Streptococcus pneumoniae is one of the most common Gram-positive pathogens that colonizes the upper respiratory tract and causes many severe infections like otitis media, sinusitis, and more life-threatening diseases like pneumonia, bacteremia, and meningitis, when it gains access to the lower respiratory tract or the bloodstream (1, 2). In the United States alone, there were in the last 20 years approximately 7 million cases of otitis media each year, 500,000 cases of pneumonia, 50,000 cases of bacteremia, and 3,000 cases of meningitis (3, 4). *S. pneumoniae* also causes a high mortality rate of 40,000 per year in the United States. When the infection has cleared, patients often retain neurological sequelae like hearing impairment or learning disabilities.

Most bacteria are surrounded by a capsule, which makes recognition by the immune system more difficult. On the basis of the differences in composition of the capsular polysaccharides, *S. pneumoniae* can be divided into >90 serotypes (5, 6). But, only seven serotypes (4, 6B, 9V, 14, 18C, 19F, and 23F) are responsible for 65% of all cases of pneumococcal disease (7) and 23 serotypes for 90% (8).

A prevalent problem with *S. pneumoniae* infections is the emergence of antibiotic-resistant strains in the last years. Previous studies show an increase in penicillin resistance of *S. pneumoniae* from 4% to 21% over a 3-year period (2), and there are some isolates that are resistant to vancomycin (9) and levofloxacin (10). A thorough understanding of the immune response to *S. pneumoniae* might open up new treatment opportunities.

Like all Gram-positive bacteria, the cell envelope of *S. pneumoniae* consists of a cell wall containing several layers of peptidoglycan with bound teichoic acids and lipoteichoic acids (LTA),[3] which are anchored in the cell membrane. According to previous reports (11, 12) the pneumococcal lipoteichoic acid has a completely different chemical structure to the well characterized LTA from *Staphylococcus aureus*. The polyglycerophosphate in the staphylococcal LTA backbone is replaced by a pentamer repeating unit composed of ribitol and a tetrasaccharide, and the phosphate content in the pneumococcal LTA is much lower than that of LTA from *S. aureus*. The LTA backbone of staphylococcal LTA carries *N*-acetyl-D-glucosamine and D-alanine, which both play a central role in the biological activity of this LTA. Instead of these substituents, phosphocholine and *N*-acetyl-D-galactosamine are found in the pneumococcal LTA (12).

The pneumococcal LTA stimulates the release of pro-inflammatory cytokines but was reported to be less potent in

* This study was supported by the German Research Council (FOR 434). The costs of publication of this article were defrayed in part by the payment of page charges. This article must therefore be hereby marked "*advertisement*" in accordance with 18 U.S.C. Section 1734 solely to indicate this fact.

[1] These authors contributed equally to this work.
[2] To whom correspondence should be addressed. Tel.: 49-7531-88-2121; Fax: 49-7531-88-4156; E-mail: Sonja.v-aulock@uni-konstanz.de.

[3] The abbreviations used are: LTA, lipoteichoic acid; LPS, lipopolysaccharide; TLR, Toll-like receptor; HIC, hydrophobic interaction chromatography; LAL, Limulus amoebocyte lysate test; LAL-F, Limulus antilipopolysaccharide factor; Gal*p*NAc, *N*-acetyl-D-galactosamine; β-Glc*p*, glucose; AATGal*p*, 2-acetamido-4-amino-2,4,6-trideoxygalactose; G-CSF, granulocyte colony-stimulating factor; IFNγ, interferon γ.

comparison to LTA from *S. aureus* (13). Activation of the monocytes occurs via the Toll-like receptor 2 (TLR-2) with CD14 as co-receptor (14).

The LTA from *S. pneumoniae* described initially was isolated by a very complex and time-consuming method (15, 16). After autolysis of the bacteria and several enzyme treatments, a co-fractionation of radioactive choline label and antigenic activity was used for the preparation of the LTA. This complex isolation procedure and the low yield of LTA were the reasons why structural studies were not performed before 1992. Using a chloroform-methanol extraction, Behr *et al.* (12) developed a simpler and more effective isolation procedure resulting in the establishment of the structure of pneumococcal LTA from strain R6 (12).

5 years ago a new isolation procedure for the LTA from *S. aureus* was published using butanol for the extraction instead of hot phenol or chloroform-methanol (17). It was shown that the previously used methods resulted in a decomposition of the LTA characterized by the loss of glycerophosphate units as well as D-alanine and *N*-acetyl-D-glucosamine substituents (18). The components of the LTA backbone seemed to play a very important role in the biological activity of the LTA as indicated by the activity of synthetic derivatives of the LTA from *S. aureus*, which induced cytokine release in human monocytes that depended on the stereoisomer of D-alanine substituents (19). Since then, LTA from further bacteria like *Bacillus subtilis*, *Streptococcus pyogenes*, *Streptococcus agalactiae*, and *Lactobacillus plantarum* (18, 20, 21) have been isolated by this method. All of these have a similar molecular structure and immunostimulatory potency.

In the present study we asked whether the butanol-extracted LTA from *S. pneumoniae* shows differences in its chemical structure in comparison to the reported chloroform-methanol-extracted LTA, possibly resulting in differences in the immunostimulatory potency of these pneumococcal LTA. For the biological characterization of the LTA we focused our interest on the cytokine induction by human whole blood, the activation of neutrophilic granulocytes, and the TLR dependence. We chose two different strains of *S. pneumoniae*, the well known laboratory R6 strain (serotype 2), which has been used in most studies since the 1950s, and the Fp23 strain (serotype 4), which was isolated in 1987 and whose complete genome sequence is published (22). The isolation and characterization of the LTA from these strains might help to elucidate the interaction between the pathogen and the immune system, giving a better insight into the pathogenesis of *S. pneumoniae*.

EXPERIMENTAL PROCEDURES

Bacterial Strains and Cultivation—*S. pneumoniae* strain R6 (serotype 2), kindly provided by E. Tuomanen, St. Jude's Children's Research Hospital, Memphis, TN, and *S. pneumoniae* strain Fp23 (serotype 4) provided by M. R. Oggioni, Dipartimento di Biologia Molecolare, Università di Siena, Siena, Italy, were grown to the late logarithmic phase (A_{580} of 0.9) in Todd-Hewitt broth (Oxoid, Milan, Italy). Bacteria were washed extensively with distilled water and lyophilized.

S. aureus (DSM 20233) was cultured aerobically and harvested after 18 h (stirring at 37 °C, 150 rpm) at an A_{578} of 3 by centrifugation at 4225 × *g* for 20 min. Integrity of bacteria and potential contaminations by Gram-negative bacterial species were checked by Gram staining and microscopy. Until the extraction, the bacteria were frozen at −20 °C.

LTA Purification—The bacteria underwent butanol extraction and hydrophobic interaction chromatography as described (17). Briefly, after resuspension in 0.05 M citrate buffer at pH 4.7, bacteria were disrupted by sonification for 15 min. The bacterial lysate (30 ml) was mixed with an equal volume of *n*-butanol (Merck, Darmstadt, Germany) under stirring for 20 min at room temperature. Centrifugation at 17,200 × *g* for 40 min resulted in a two-phase system, and the lower, aqueous phase was collected before the addition of fresh citrate buffer for a second extraction. This re-extraction was performed twice, and the three aqueous phases were pooled and lyophilized. After resuspension of the sample in 35 ml of chromatography start buffer (15% *n*-propanol in 0.1 M ammonium acetate, pH 4.7), it was centrifuged at 26,900 × *g* for 60 min and filtered (0.2 μm). The supernatant was subjected to hydrophobic interaction chromatography (HIC) on an octyl-Sepharose column (2.5 × 11 cm) using a linear gradient from 15% to 60% *n*-propanol in 0.1 M ammonium acetate (pH 4.7).

LTA Dealanylation—7.9 mg of LTA Fp23 in Tris buffer (1.25 M in MilliQ, pH 8.5) was stirred at 500 rpm for 24 h at room temperature. After lyophilization the sample was purified by HIC as described above. The absence of D-alanine in the LTA Fp23 was confirmed by NMR analysis.

Phosphate Determination—This method is based on the formation of phosphomolybdenum blue from phosphate. 50 μl of a phosphate standard (0.65 mM, Sigma), and 100 μl of each fraction was mixed with 200 μl of ashing solution (2 M H_2SO_4 and 0.44 M $HClO_4$) and incubated in open polypropylene vials (Eppendorf, Hamburg, Germany) at 145 °C for 2.5 h. Then 1 ml of reducing solution was added containing 3 mM ammonium molybdate, 0.25 M sodium acetate, and 1% ascorbic acid. After 2 h at 45 °C, 250 μl of each sample was transferred to flat-bottom, ultrasorbant 96-well plates (Nunc, Wiesbaden, Germany), and the absorption was measured in an ELISA Reader (Rainbow, Tecan, Crailsheim, Germany) at 700 nm. The LTA containing fractions were pooled, and the endotoxin contamination of the LTAs was assessed by the kinetic Limulus amoebocyte lysate assay (Charles River, Charleston, SC).

Whole Blood Incubation—Human whole blood incubations were performed as described previously (23). Briefly, human blood was drawn from healthy volunteers into heparinized S-monovettes® (Sarstedt, Nümbrecht, Germany) and diluted 5-fold in RPMI 1640 medium (Biochrom, Berlin, Germany). The following stimuli and inhibitors were used: 50 μl of each chromatography fraction, which had been evaporated and resuspended in 50 μl of 0.9% NaCl, LPS from *Salmonella abortus equi* (Sigma), LTA from *S. aureus* (LTA Sa), LTA from *Streptococcus pneumoniae* strain R6 (LTA R6) and strain Fp23 (LTA Fp23), which all were isolated in-house by *n*-butanol extraction, Zymosan A from *Saccharomyces cerevisiae* (Sigma), and polymyxin B (Sigma) and Limulus antilipopolysaccharide factor LAL-F (a generous gift from F. Jordan, Charles River).

The final volume was adjusted to 500 μl. Incubations were carried out in open polypropylene vials overnight for 22 h at 37 °C and 5% CO_2. The pelleted blood cells were then resuspended by gentle shaking and were centrifuged at 400 × *g* for 2 min. The cell-free supernatants were stored at −80 °C until cytokine measurement by ELISA.

Isolation of Human Neutrophilic Granulocytes and Determination of the Myeloperoxidase Activity—Neutrophils were obtained with a Percoll gradient (BD Biosciences) as described (24). After the centrifugation of heparinized blood at 270 × *g* for 20 min, the resulting buffy coat was mixed with 0.72% dextran T500 (Sigma) in 50 ml of phosphate-buffered saline. 30 min later the erythrocytes had sedimented. The supernatant contained leukocytes, which were centrifuged at 850 × *g* for 7 min and washed once with HEPES buffer. The cells were transferred to a discontinuous Percoll/HEPES buffer gradient (density 1.093, 1.088, 1.072, and 1.059) and spun for 15 min at 450 × *g*. The neutrophil band was transferred to a new tube and was washed once with HEPES buffer at 850 × *g* for 7 min. Afterward differential cell counts were determined with a Pentra60 (ABX Diagnostics, Montpellier, France), and the cells were diluted to 5×10^6 cells/ml with RPMI 1640 medium (Biochrom) and 10% autologous serum. Finally the neutrophilic granulocytes were plated to 96-well culture plates (5×10^5 cells/well, Greiner, Nürtingen, Germany) and were incubated with different stimuli for 22 h at 37 °C and 5% CO_2.

50 μl of a potassium buffer (50 mM, pH 6.0) containing EDTA (10 mM) and 0.5% (w/v) hexadexylammonium bromide (both Sigma) were added to the supernatants of the incubations. Myeloperoxidase from human leukocytes (Sigma) served as the standard. After the addition of 3,3′,5,5′-tetramethylbenzidine (Sigma), the activity of the myeloperoxidase could be determined. The reaction was stopped by the addition of H_2SO_4, and the absorption was measured at 450 nm.

Isolation of Murine Bone Marrow Cells—C3H/HeJ mice, characterized by a non-functional TLR4, and the corresponding wild-type mouse strain C3H/HeN were purchased from Charles River Laboratories. TLR2-deficient mice kindly provided by Tularik (South San Francisco, CA) and the corresponding wild-type mice (129Sv/B57BL/6) were bred in the animal facilities of the University of Konstanz and genotyped. Mice were killed by terminal pentobarbital anesthesia (Narcoren, Merial, Halbergmoos, Germany). The humeri and femurs of the mice were lavaged with 10 ml of ice-cold sterile phosphate-buffered saline (Invitrogen). The lavages were transferred to siliconized glass tubes (Vacutainer, Bioscience, Heidelberg, Germany), and bone debris was removed. After one centrifugation step the cell counts were determined. The cells were diluted to 5×10^6/ml with RPMI 1640 supplemented with 10% heat-inactivated fetal calf serum (Biochrom), 100 IU/ml penicillin/streptomycin (both from Biochrom), and plated to 96-well culture plates for stimulation with different stimuli. After 22 h at 37 °C, 5% CO_2 supernatants were frozen at −80 °C until cytokine measurement by ELISA.

Cytokine Measurement—Cytokines released by human whole blood were measured by in-house sandwich ELISA using commercially available antibody pairs and recombinant standards. Monoclonal antibody pairs against human TNF, IL-8, and IFNγ were purchased from Endogen (Perbio Science, Bonn, Germany), against human IL-1β and G-CSF from R&D (Wiesbaden, Germany), and against human IL-10 from BD Biosciences. Recombinant standards for TNF and IL-1β were kind gifts from S. Poole (National Institute for Biological Standards and Control, Herts, UK), rIL-8 from PeproTech (Tebu, Frankfurt, Germany), rIFNγ from Thomae (Biberach, Germany), rG-CSF from Amgen (Thousand Oaks, CA), and rIL-10 from BD Biosciences. The release of murine TNF by bone marrow cells was measured with the DuoSet-kit from R&D. Assays were carried out in flat-bottom, ultrasorbant 96-well plates. The secondary biotinylated antibodies were detected by horseradish-peroxidase-conjugated streptavidin (BIOSOURCE, Camarillo, CA), and 3,3′,5,5′-tetramethylbenzidine (Sigma) was used as substrate. The reaction was stopped with 1 M H_2SO_4, and the absorption was measured in an ELISA reader at 450 nm with a reference wavelength of 690 nm.

NMR Spectroscopy—NMR spectra were obtained on a Bruker Avance 600 spectrometer at 300 K using sample tubes with a 5-mm outer diameter. Spectra were measured for solutions in D_2O using sodium 3-trimethylsilyl-3,3,2,2-tetradeuteropropanoate as an internal standard for ^1H NMR (δ_H 0.00 ppm) and acetone for ^{13}C NMR (δ_C 30.02 ppm). For ^{31}P NMR spectra 2% phosphoric acid was used as external standard ($\delta_P = 0.00$ ppm).

Two-dimensional homonuclear DFQ-COSY, TOCSY, NOESY, and ROESY experiments and two-dimensional heteronuclear HMQC and HSQC (^1H-^{13}C) were performed using standard Bruker pulse programs. TOCSY, NOESY, and ROESY experiments were performed in the phase-sensitive mode using mixing times of 100 ms in the TOCSY and 200-ms spinlock for NOESY and ROESY.

Statistics—Statistical analysis was performed using the GraphPad Prism program (GraphPad Software, San Diego, CA). Data are shown as means ± S.E. For statistical analysis of two groups of non-parametric data, Wilcoxon matched pairs test (human data) and unpaired Student's *t* test (mouse data) were used. Repeated-measure analysis of variance was assessed using the one-way analysis of variance test followed by the Bonferroni multiple comparison test (Figs. 3 and 13). A p value <0.05 was considered significant. In the figures *, **, and *** represent p values <0.05, <0.01, and <0.001, respectively. Cytokine levels are given per milliliter blood, *i.e.* corrected for the dilution factor 5 in the 20% blood incubation.

RESULTS

LTA Purification by Hydrophobic Interaction Chromatography—After the butanol extraction of *S. pneumoniae* the aqueous phase was subjected to hydrophobic interaction chromatography. The resulting fractions were screened for phosphate content. For both strains of *S. pneumoniae* we obtained high phosphate contents in the flow-through fractions (fractions 1–19), representing DNA and proteins that had not bound to the chromatography column, and a second peak from fraction 43 to 50, corresponding to the fractions that yield LTA upon extraction of *S. aureus* (Fig. 1, *A* and *B*). We screened the fractions for IL-8 induction in human whole blood. The resulting profile of the IL-8-induction by the fractions from strain R6 (Fig. 1*A*) was congruent with that of the Fp23 strain fractions as

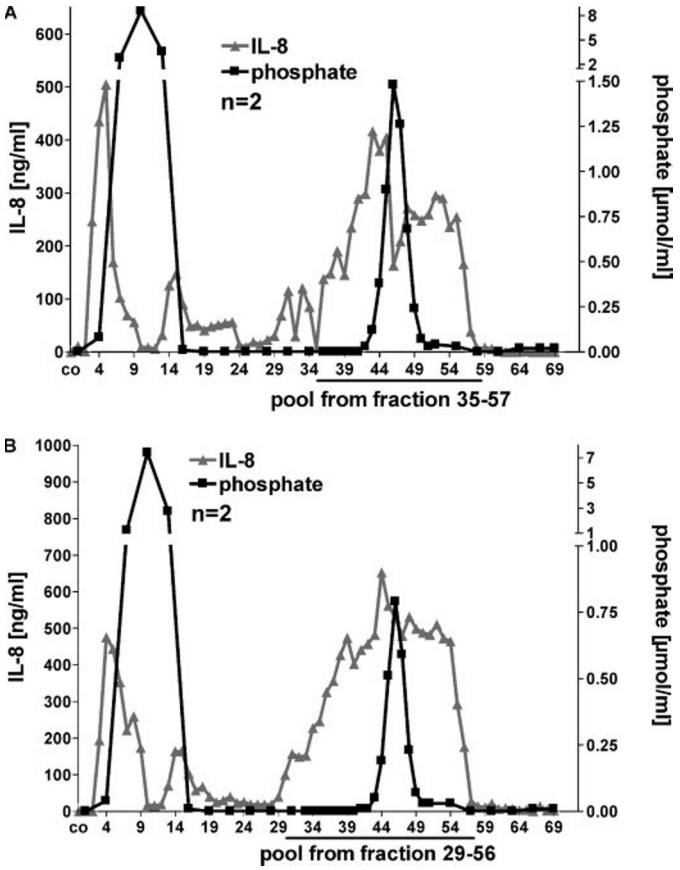

FIGURE 1. **Screening of HIC fractions after butanol extraction.** After butanol extraction of *S. pneumoniae* R6 (*A*) and Fp23 (*B*) the HIC-fractions were screened for phosphate content and IL-8 induction in human whole blood. The cytokine release was determined after 22 h in the cell-free supernatants by ELISA. The mean profile of two blood donors is shown.

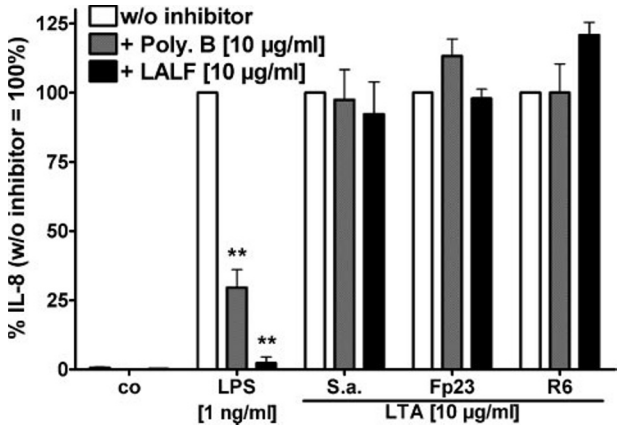

FIGURE 2. **Exclusion of LPS contamination in LTA Fp23 and LTA R6 preparations.** Human whole blood from four healthy volunteers was incubated in the presence of 1 ng/ml LPS and 10 μg/ml LTA from *S. aureus*, *S. pneumoniae* Fp23, and R6 for 22 h. Saline, 10 μg/ml polymyxin B, or LAL-F were added to each stimulus. IL-8 was measured in the cell-free supernatants by ELISA. Data are means $\pm$ S.E., given as percent inhibition.

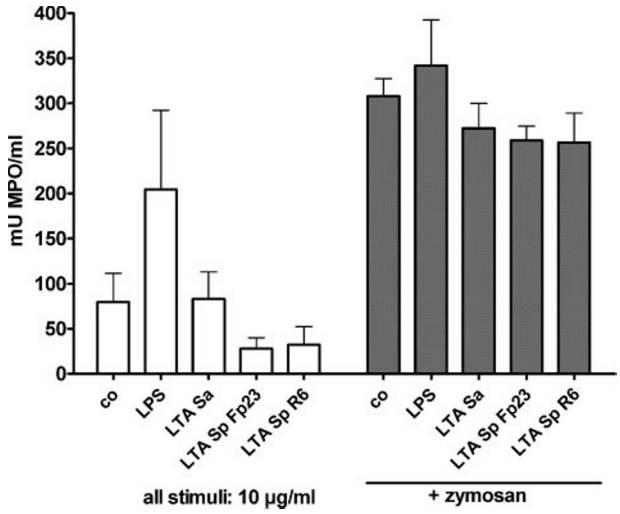

FIGURE 3. **Neutrophilic granulocytes induce no myeloperoxidase release after stimulation with LTA.** Isolated neutrophils (5×10^5/well) from five healthy volunteers were incubated for 22 h in the presence of LPS, LTA from *S. aureus*, LTA Fp23, LTA R6, and zymosan and a combination of either stimulus with zymosan. Myeloperoxidase release was measured in the cell-free supernatant as 3,3′,5,5′-tetramethylbenzidine turnover. All stimuli *versus* respective control, not significant; control without zymosan *versus* control with zymosan, $p < 0.001$ (Bonferroni multiple comparison test).

shown in Fig. 1*B*, whereas in both cases the peaks were broader than the phosphate peaks (pooled fractions: 30–57) as expected due to the higher sensitivity of the human whole blood assay compared with the phosphate measurement. The screening profiles shown are representative for two extractions of the R6 strain and nine extractions of the Fp23 strain.

Exclusion of LPS Contamination in LTA Fp23 and LTA R6 Preparations—To exclude an LPS contamination we used different inhibitors and the Limulus amoebocyte lysate (LAL) test. Polymyxin B is an inhibitor for negatively charged molecules like LPS. LAL-F inhibits endotoxin-induced signals more specifically than polymyxin B by binding to the Lipid A portion (25).

As expected, LPS-induced IL-8 release was reduced to 25 and 2% by Polymyxin B and LAL-F, respectively, showing the efficiency of the inhibitors. The cytokine release induced by LTA *S. aureus*, LTA Fp23, and LTA R6, respectively, were influenced neither by polymyxin B nor by LAL-F (Fig. 2). The results from these experiments were confirmed by the LAL showing for all LTA extractions an LPS contamination below 2 endotoxin units/mg of LTA, *i.e.* <200 pg LPS per mg.

Neither LTA Fp23 nor LTA R6 Activate the Release of Myeloperoxidase by Neutrophilic Granulocytes—Knowing that LTA from *S. aureus* does not induce myeloperoxidase release from neutrophilic granulocytes, we investigated whether this also holds true for pneumococcal LTA. Zymosan, a well known activator of myeloperoxidase release, was used as a positive control. LPS alone was able to stimulate the neutrophilic granulocytes. Myeloperoxidase release was not induced by LTA, and LTA had no effect on the zymosan spike (Fig. 3).

Pneumococcal LTA Is TLR2- and Not TLR4-dependent—To test the TLR dependence of the pneumococcal LTAs, we stimulated bone marrow cells from $TLR2^{+/+}$ and $TLR2^{-/-}$ mice (Fig. 4*A*). As expected 1 ng/ml LPS induced similar amounts of TNF in cells from wild-type and $TLR2^{-/-}$ mice. However, 10 μg/ml *S. aureus* LTA, a known TLR2 agonist, exclusively induced measurable TNF amounts in cells from TLR2 wild-type mice. The stimulation of $TLR2^{+/+}$ wild-type cells with LTA Fp23 and LTA R6 (each 10 μg/ml) resulted in comparable TNF release, whereas the cells from $TLR2^{-/-}$ mice did not

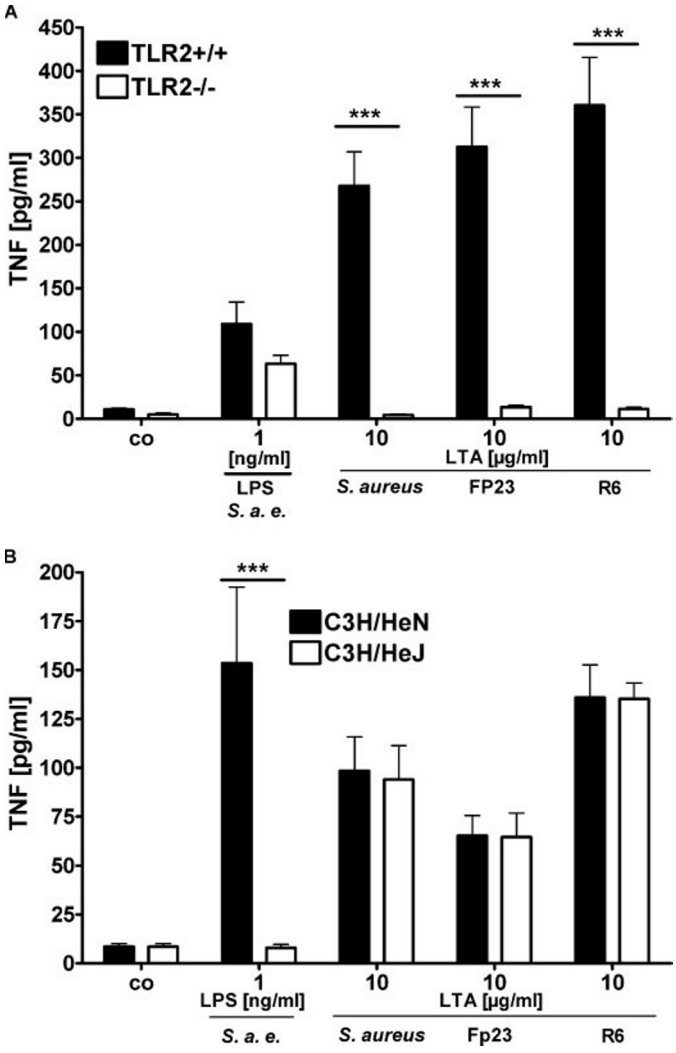

FIGURE 4. **TLR dependence of staphylococcal and pneumococcal LTA.** TNF response of bone marrow cells derived from TLR-$2^{+/+}$ (*black bars*) and TLR-$2^{-/-}$ (*white bars*) mice (*A*) with $n = 5$ or from TLR4 wild-type mice (C3H/HeN, *black bars*) and mice (C3H/HeJ) with a non-functional TLR4 receptor (*white bars*) (*B*) with $n = 8$ to stimulation with 1 ng/ml LPS and 10 μg/ml purified LTA, respectively. Data are means ± S.E.

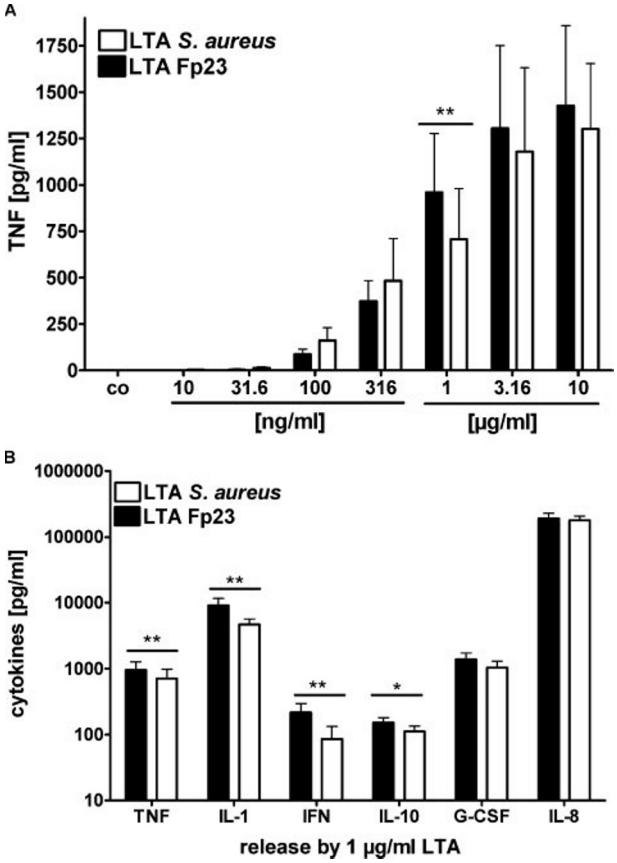

FIGURE 5. **Comparison of cytokine induction by LTA from *S. aureus* and *S. pneumoniae* Fp23.** Human whole blood from 11 healthy volunteers was stimulated with the given concentrations of either LTA for 22 h. *A*, TNF release was measured in the cell-free supernatants by ELISA. *B*, from the same incubations all shown cytokines were measured by ELISA and plotted for 1 μg/ml stimulus concentration. The detection limits for all cytokine ELISA were between 1 and 15 pg/ml. The cytokine release by the unstimulated controls was below this detection limit for every cytokine measured. Data are means ± S.E.

respond to these stimuli, showing TLR2 dependence of the pneumococcal LTA. The results of the stimulation of TLR4 wild-type cells and cells with a non-functional TLR4 receptor (Fig. 4*B*) showed no difference in the cytokine release of both cell types after stimulation with LTA Fp23 and LTA R6.

LTA Fp23 Is as Potent as LTA from S. aureus in Inducing Different Cytokines—We compared the cytokine release induced by LTA from *S. aureus* and LTA Fp23. Human whole blood was stimulated with increasing concentrations of either LTA (from 10 ng/ml to 10 μg/ml), and the cytokine release was measured by ELISA. Comparing the TNF release, the LTAs were equipotent at each concentration (Fig. 5*A*). From the same samples we measured further cytokines and chemokines. With 10 μg/ml there was a high IL-8 (300 ng/ml) and IL-1 induction (10 ng/ml) by both LTAs. The G-CSF release (2000 pg/ml) was similar to the TNF induction (1600 pg/ml), and there was only a very low IFNγ (600 pg/ml) and IL-10 (200 pg/ml) release (data not shown). The induced cytokine release by the LTA from *S. aureus* at 1 μg/ml was compared with the corresponding cytokine induction by LTA Fp23 at 1 μg/ml. Fig. 5*B* shows that LTA Fp23 induced all measured cytokines and chemokines at nearly the same level or even at significantly higher levels compared with LTA from *S. aureus*.

LTA R6 Is a Weaker Cytokine Inducer than LTA Fp23—Next we compared the LTA from the two pneumococcal strains. Both LTAs were able to stimulate TNF release, but LTA Fp23 showed a significantly higher TNF induction compared with LTA R6 (Fig. 6*A*). We observed the same lower activity of LTA R6 on the level of further cytokines. At the concentration of 1 μg/ml the LTA R6 induced only 50% of the G-CSF and IL-8 release compared with LTA Fp23. For TNF, IL-1, IL-10, and IFNγ the cytokine release by LTA R6 was reduced to 20–30% of that of LTA Fp23 (Fig. 6*B*).

NMR Analysis of LTA R6 Indicates N-Acetyl-D-galactosamine Substituent at the Ribitol—Fischer *et al.* characterized LTA structures isolated from different Gram-positive bacteria, including *S. pneumoniae* strain R6, by chemical degradation methods (12, 26–28). Yet, chemical manipulations may unintentionally cleave labile substituents resulting in a loss of structural information. The advance in the field of high resolution NMR in recent years allows the analysis of native LTA with an estimated mass between 5 and 10 kDa. How-

ever, structural investigations of lipoteichoic acid are still a challenge because microheterogeneity of the fatty acid chain, the length of the repeating unit, the glycosylation, and alanylation pattern makes a complete assignment of native lipoteichoic acid nearly impossible.

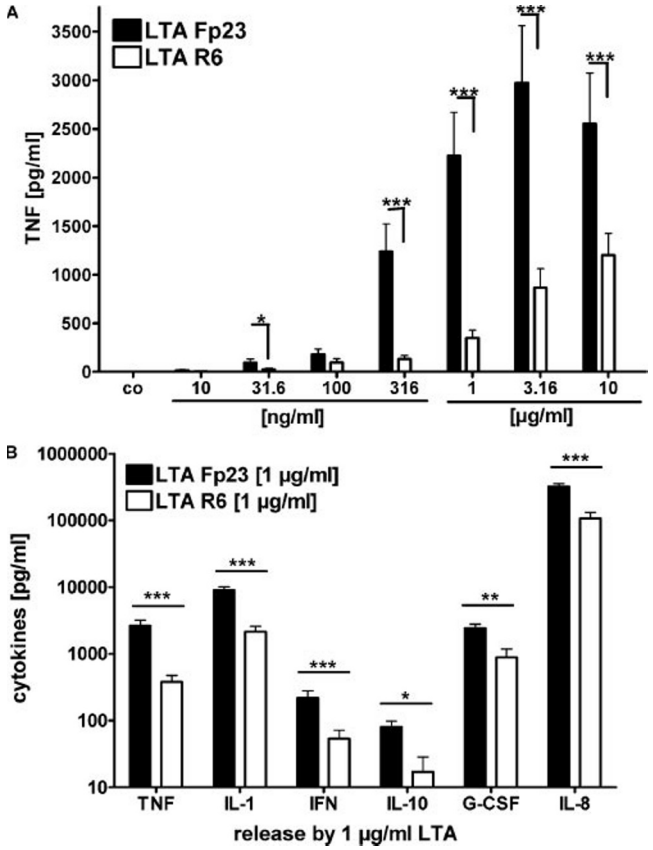

FIGURE 6. **Comparison of cytokine induction by LTA from *S. pneumoniae* Fp23 and R6.** Human whole blood from 12 healthy volunteers was stimulated with the given concentrations of either LTA for 22 h. *A*, TNF release was measured in the cell-free supernatants by ELISA. *B*, from the same incubations all shown cytokines were measured by ELISA and plotted for 1 μg/ml stimulus concentration. The detection limits for all cytokine ELISA were between 1 and 15 pg/ml. The cytokine release by the unstimulated controls was below this detection limit for every cytokine measured. Data are means ± S.E.

For assignment of the proton signals, 2D TOCSY and 2D DQF-COSY experiments with water suppression technique were used, and HSQC experiments were used for the ^{13}C chemical shifts. Due to the small $^{3}J_{H3,H4}$ and $^{3}J_{H4,H5}$ of Gal*p*NAc, a few signals of these sugars remained unassigned, and some signals of the ribitol unit could not be determined due to overlap (Table 1). The structure is summarized in Fig. 7. The chemical shifts for the pentamer repeating unit are in good agreement with data regarding similar structures (29–32).

The ^{1}H NMR of strain R6 showed five anomeric signals, of which the four signals of same intensity at δ_H 4.61, 4.63, 4.97, and 5.17, belong to the tetrasaccharide of the repeating unit. The signal with smaller intensity at δ_H 5.09 originates from partial glycosylation of ribitol with α-Gal*p*NAc. From the ^{1}H NMR integrals the degree of substitution with α-Gal*p*NAc was determined to be ~40%, and the average length of the LTA with $n = 2–3$ of the repeating pentamer was also calculated from the proton spectrum (Fig. 8*A*).

The connectivity of the polysaccharide repeating unit was determined by 2D NOESY and 2D ROESY experiments with water suppression. The use of an HMBC spectrum was not possible because of the low sample concentration. The *syn* conformation of the glycosidic linkage causes a strong NOE between the two protons on both sides of the glycosidic bond. This NOE is observed as the most intensive trans-glycosidic signal and is particularly suited to identify the sequence of the pentamer. The inter-residue NOE contact between H-1 of the β-Glc*p* residue and H-3 of 2-acetamido-4-amino-2,4,6-trideoxy-galactose (AATGal*p*) identifies the A-B linkage. The B-C structural element is established with an NOE contact between the H-1 of AATGal*p* and H-4 of α-Gal*p*NAc. Furthermore the linkage between residues C and D is characterized by the dipolar correlation of the α-anomeric proton of Gal*p*NAc with H-3 of β-Gal*p*NAc. A cross-peak in the NOE spectrum between H-1 of β-Gal*p*NAc and the methylene group of ribitol demonstrates the structural element D–E.

The glycosylation of ribitol with α-Gal*p*NAc (marked with "*X*" in the spectra) is identified from NOEs between the ano-

TABLE 1
^{1}H NMR and ^{13}C NMR data for the LTA from *S. pneumoniae* strain R6

Sugar residues[a]	Chemical shifts for						
	1	2	3	4	5	6	NAc
A: →6)-β-Glc*p*-(1→	4.63	3.35	3.51	3.52	3.58	4.11, 4.16	
	104.7	73.5	76.0	69.4	75.1	64.9	
B: →3)-α-AATGal*p*-(1→	4.97	4.22	4.40	3.99	4.79	1.24	2.09
	98.9	48.9	75.3	55.4	63.6	16.2	23.1
C: →4)-α-Gal*p*NAc-(1→	5.17	4.32	3.94	4.11	ND[b]	4.01	2.11
6	94.1	50.0	67.4	77.3		64.2	22.8
↑							
D: →3)-β-Gal*p*NAc-(1→	4.61	4.10	3.87	4.18	3.84	~4.07	2.06
6	101.9	51.3	75.4	63.9	74.2	65.2	22.8
↑							
E (unsubstituted): →1)-Ribitol-5-*P*-(O→	3.89, 3.99	—[c]	ND[b]	—[c]	3.99, 4.06		
	71.2				67.3		
X: α-Gal*p*NAc-(1→	5.09	4.23	3.81	4.05	ND[b]	3.78, 3.84	2.05
	94.2	50.0	68.3	68.7		61.7	~22.8
At C: Cho-*P*-(O→	4.29	3.67	3.24				
	60.2	66.7	54.7				
At D: Cho-*P*-(O→	4.34	3.69	3.24				
	60.2	66.7	54.7				

[a] Where AATGal is 2-acetamido-4-amino-2,4,6-trideoxygalactose, and all sugars belong to the D-series.
[b] ND, not determined.
[c] 3.77/77.1, not resolved

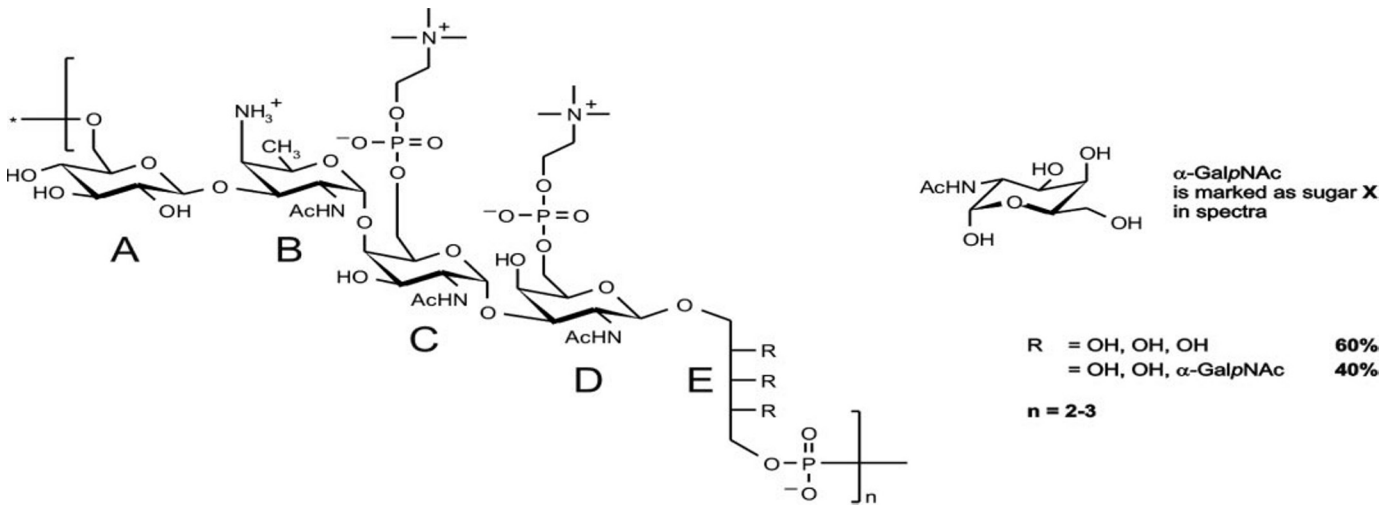

FIGURE 7. **Structure and substitution pattern of the repeating unit of LTA isolated from *S. pneumoniae* strain R6.** The percentage of glycosylation and the average number of the repeating units was determined from the ^{1}H NMR spectrum.

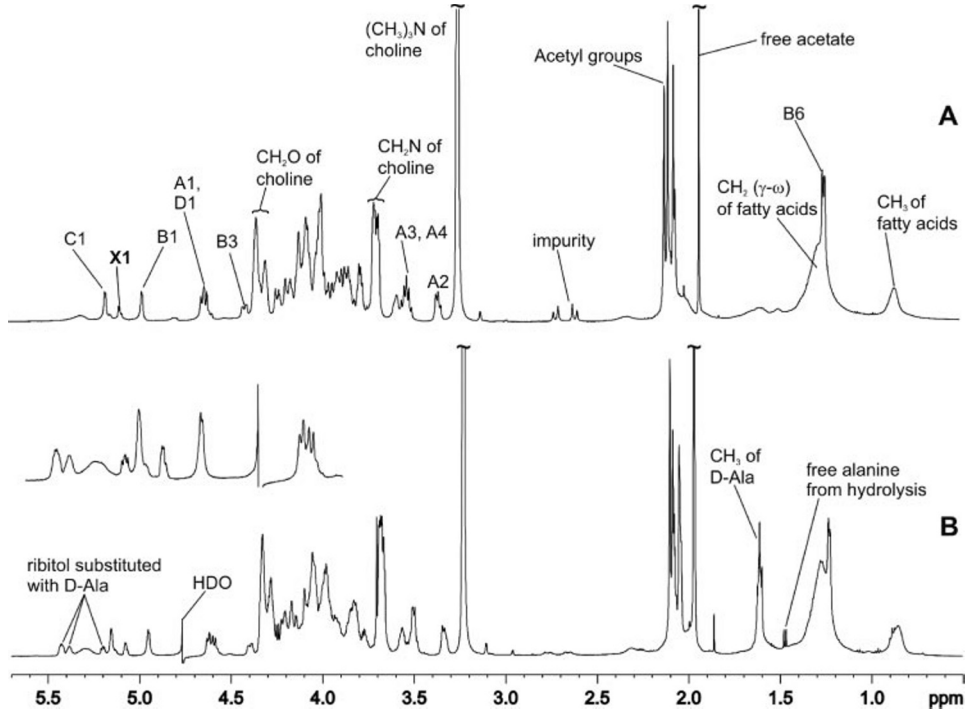

FIGURE 8. **Comparison of ^{1}H NMR spectra of LTA from *S. pneumoniae* Fp23 and R6.** ^{1}H NMR (600 MHz and 300 K) with water suppression of LTA isolated from *S. pneumoniae* strain R6 (*A*) and *S. pneumoniae* strain Fp23 (*B*). The additional alanylation in the LTA from Fp23 is marked at 1.6 ppm.

meric proton (δ_H 5.09) and δ_H 4.16, 4.12, and 3.83. A single doublet at δ_H 5.09 suggests that glycosylation occurs at a single O of the ribitol unit, but we could not resolve which of the three secondary hydroxyls was glycosylated.

Four different signals could be observed in the ^{31}P NMR spectrum of strain R6 (data not shown), which were assigned by comparison with literature data (12, 26–28). The three signals at δ_P −0.79, −0.31, and 1.28 were approximately of the same intensity and belong to phosphocholine groups (δ_P −0.79 and −0.31), indicating that position 6 of each residue C and D were substituted with a phosphatidylcholine, and the signal at δ_P 1.28 was assigned to the ribitol phosphate. The small signal at δ_P −0.52 originated from the terminal repeating unit. The micellar structure of native lipoteichoic acid in aqueous solution leads to line broadening in the ^{1}H NMR, especially in the region of the membrane anchor, which could not be further analyzed by NMR methods.

LTA Fp23 Carries D*-Alanine Bound to Ribitol, but LTA R6 Does Not*—The structure of the unsubstituted repeating unit of Fp23 was determined to be the same as for the lipoteichoic acid from strain R6, with chemical shift variations below 0.02 ppm for proton shifts and below 0.1 ppm for ^{13}C (Table 2).

However, an important difference between the LTA from strain R6 and Fp23 can already be observed in the ^{1}H NMR spectra (Fig. 8). The additional signals occurring in the spectrum of Fp23 at δ_H 1.61, 5.20, 5.38, and 5.42 were assigned to D-alanine linked to the ribitol of the repeating unit. The signal at δ_H 1.61 belongs to the methyl group of D-alanine and shows ^{3}J coupling in the DQF-COSY to H-α of the amino acid at δ_H 4.25. From HSQC spectrum ^{13}C shifts for the CH_3 group (δ_C 15.8) and for the methine proton (δ_C 49.5) were obtained. The three signals at δ_H 5.20, 5.38, and 5.42 with identical intensity are assigned to the three methine protons of ribitol, which is substituted with D-alanine. Each ribitol is substituted by not more than one D-alanine, but the position of alanylation varies in different repeating units or LTA molecules (Fig. 9).

An NOE contact between the methyl group and methine protons at δ_H 5.20, 5.38, and 5.42 confirms this assignment. The corresponding carbon shifts can be observed at δ_C 76.0, 76.2, and 76.3, respectively (Fig. 10).

TABLE 2
^{1}H NMR and ^{13}C NMR data for the LTA from *S. pneumoniae* strain Fp23

Sugar residues[a]	Chemical shifts for						
	1	2	3	4	5	6	NAc
A: →6)-β-Glc*p*-(1→	4.63	3.34	3.50	3.51	3.57	4.09, 4.14	
	104.7	73.4	76.0	69.4	75.0	64.9	
B: →3)-α-AATGal*p*-(1→	4.95	4.22	4.40	3.98	4.77	1.23	2.09
	98.8	48.9	75.3	55.4	63.6	16.1	23.1
C: →4)-α-Gal*p*NAc-(1→	5.12	4.32	3.92	4.10	ND[b]	4.00	2.10
6	94.0	50.0	67.4	77.2		64.1	22.7
↑							
D: →3)-β-Gal*p*NAc-(1→	4.59	4.09	3.85	4.15	3.82	~4.06	2.05
6	101.9	51.3	75.3	63.9	74.1	65.1	22.7
↑							
E (unsubstituted): →1)-Ribitol-5-*P*-(O→	3.88, 3.98	—[c]	ND[b]	—[c]	3.98, 4.05		
	71.2				67.2		
X: α-Gal*p*NAc-(1→	5.08	4.22	3.80	4.04	ND[b]	3.77, 3.83	ND[b]
	94.2	50.0	68.2	68.6		61.7	
At C: Cho-*P*-(O→	4.28	3.67	3.23				
	60.1	66.6	54.6				
At D: Cho-*P*-(O→	4.33	3.69	3.23				
	60.2	66.6	54.6				

[c] Where AATGal is 2-acetamido-4-amino-2,4,6-trideoxygalactose, and all sugars belong to the D-series.
[b] ND, not determined.
[c] 3.77, 77.1, not resolved.

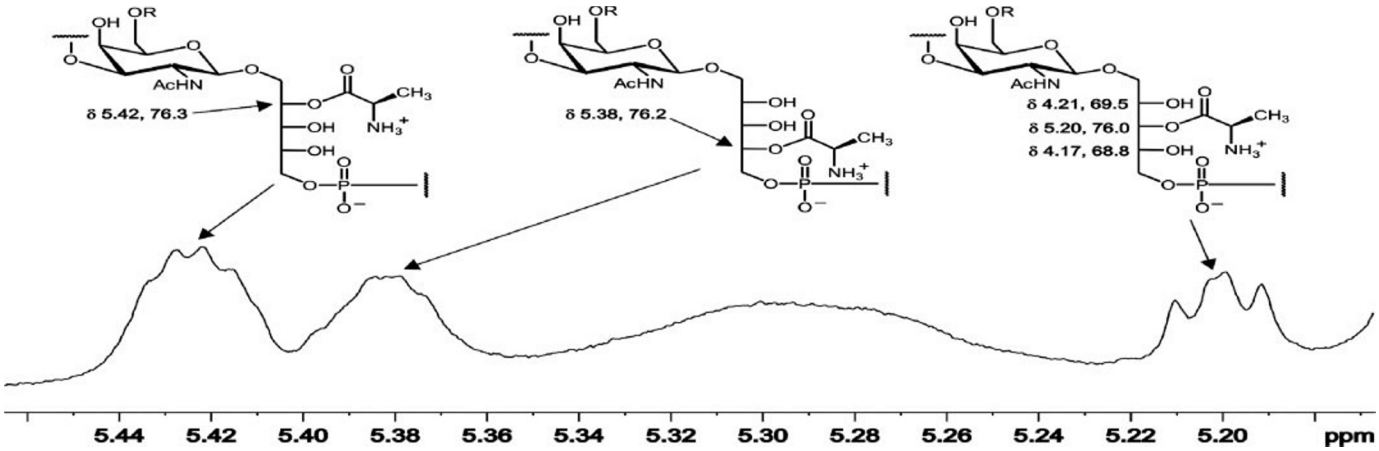

FIGURE 9. **Position of the D-alanine at the ribitol of LTA Fp23.** Assignment of the methine protons of ribitol substituted with alanine on different positions. The methine protons at position 2 and 4 could be determined for alanylation of ribitol in position 3.

Integration of these protons in ^{1}H NMR results in a nearly 1:1:1 ratio of the integrals and indicates that D-alanine is equally distributed over all three positions of the ribitol unit. This is explained by taking into account that the quite reactive D-alanyl ester migrates via the cyclic *ortho* ester intermediate from one position to the other as depicted in Fig. 11 (33, 34). As a further conclusion each ribitol moiety is either glycosylated with α-Gal*p*NAc or alanylated but does not bear both substituents together. The structure of the repeating unit of pneumococcal lipoteichoic acid isolated from Fp23 strain is summarized in Fig. 12.

From the integrals of the ^{1}H NMR of Fp23 in Fig. 8*B* the average chain length for this LTA was determined to be $n = 2$ with alanylation at almost every ribitol that is not glycosylated. The occurrence of free D-alanine at δ_H 1.47 and δ_C 16.7 for the methyl group and δ_H 3.78 and δ_C 51.1 for the H-α generated from hydrolysis of the labile D-alanine esters indicates that the D-alanine content is more likely to be underestimated.

D-Alanine Determines the Potency of the Pneumococcal LTA—To prove that the greater potency of LTA Fp23 over LTA R6 is determined by its D-alanine substituents we subjected LTA Fp23 to alkaline hydrolysis at pH 8.5. NMR confirmed that the resulting LTA lacked D-alanine but was otherwise intact. The dealanylated LTA Fp23 was used as stimulus in comparison to LTA Fp23 and LTA R6. Human whole blood was stimulated with increasing concentrations of either LTA (from 10 ng/ml to 10 μg/ml). As expected, the dealanylated LTA Fp23 induced TNF release comparable to LTA R6 and lower than the intact LTA Fp23 (Fig. 13).

DISCUSSION

S. pneumoniae is one of the most common Gram-positive pathogens. It is well known that the major virulence factors of *S. pneumoniae* are the capsule and its polysaccharides, because encapsulated strains were found to be at least 10^5 times more virulent than strains lacking the capsule (35) like most laboratory strains (R6 and Fp23). However, several studies show that patients have more LTA in their cerebrospinal fluid after treatment of *S. pneumoniae* infections with low concentrations of antibiotics than before and that this increases the neurological sequelae and the mortality rate (36, 37). So it is important to investigate the inflammatory potency of this LTA. Perhaps

structural differences in the LTA molecules of two strains can explain differences in their pathogenicity. To isolate an immunoreactive and pyrogen-free LTA from *S. pneumoniae* strain Fp23 and R6, butanol extraction and hydrophobic interaction chromatography were carried out.

Firstly we focused our interest on the immunostimulatory potency of the pneumococcal LTA from R6 and Fp23 in comparison to the LTA from *S. aureus*. The biological activity of the staphylococcal LTA is characterized by a strong release of chemoattractant factors like LTB_4 and IL-8 (24). However, although they are a strong stimulus for the recruitment of phagocytes, they do not seem to activate the neutrophilic granulocytes directly, because no oxidative burst and no release of myeloperoxidase could be measured after stimulation with LTA from *S. aureus* (24). We obtained the same results with both pneumococcal LTAs. So the recruitment, but not the activation of phagocytes, seems to be a common feature for all LTA.

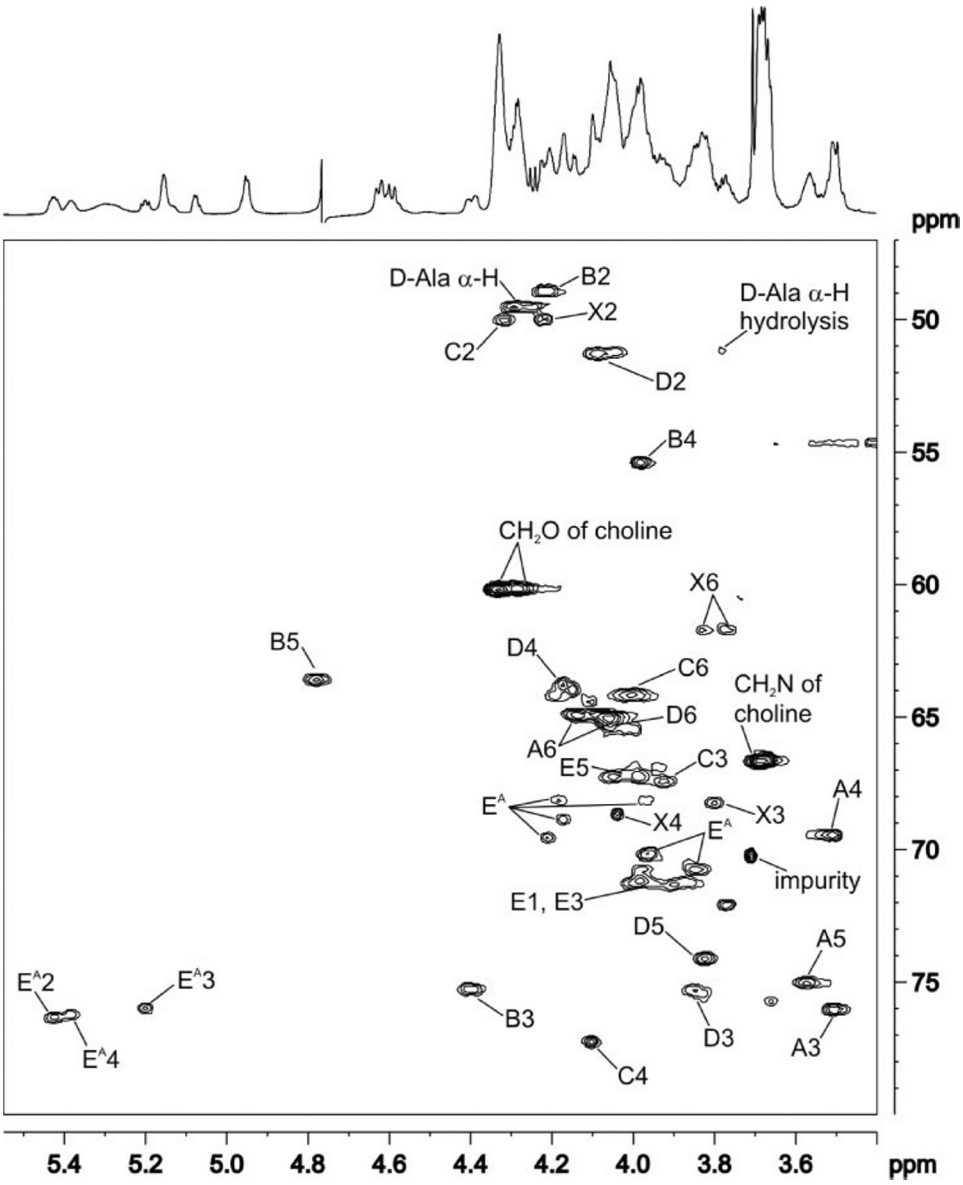

FIGURE 10. **Two-dimensional NMR analysis of LTA Fp23.** HSQC spectrum (D_2O, 600 MHz, and 300 K) of LTA isolated from *S. pneumoniae* strain Fp23. Signals from ribitol moieties substituted with alanine are marked as E^A.

According to the literature, LTA from *S. aureus* binds to TLR-2 and CD14. After the accumulation in lipid rafts, this complex is subsequently internalized and the intracellular signal cascade starts (38). For *S. pneumoniae* it was shown that TLR-2 deficient mice were highly susceptible to meningitis, which was caused by a clinical isolate of *S. pneumoniae* serotype 3 (39). Additionally, the chloroform-methanol extracted LTA from *S. pneumoniae* strain R36A stimulated peripheral blood mononuclear cells via TLR-2 and with CD14 and TLR-1 as co-receptors (13). In line with these results, the pneumococcal LTAs from strain R6 and Fp23 were both TLR-2-dependent in experiments with bone marrow cells from wild-type and $TLR2^{-/-}$ mice.

Despite the known differences in the chemical structure, staphylococcal LTA and the LTA from Fp23 were nearly equipotent in inducing six different cytokines in human whole blood. Because the pneumococcal LTA has a lower molecular mass than the LTA from *S. aureus*, the significantly higher cytokine release by LTA Fp23 would be less pronounced when used at equimolar concentrations. But the LTA from R6 showed a significantly weaker biological activity regarding all cytokines tested. So far all studies have described pneumococcal LTA

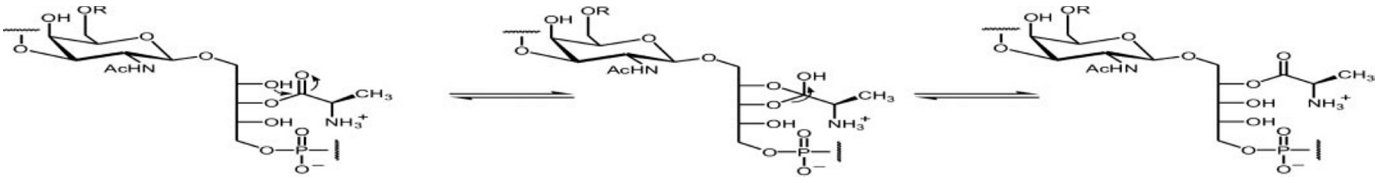

FIGURE 11. **Migration of the D-alanine at the ribitol.** Migration of the reactive alanyl ester via the cyclic *ortho* ester intermediate within one ribitol unit. D-Alanine does not migrate between different ribitol moieties.

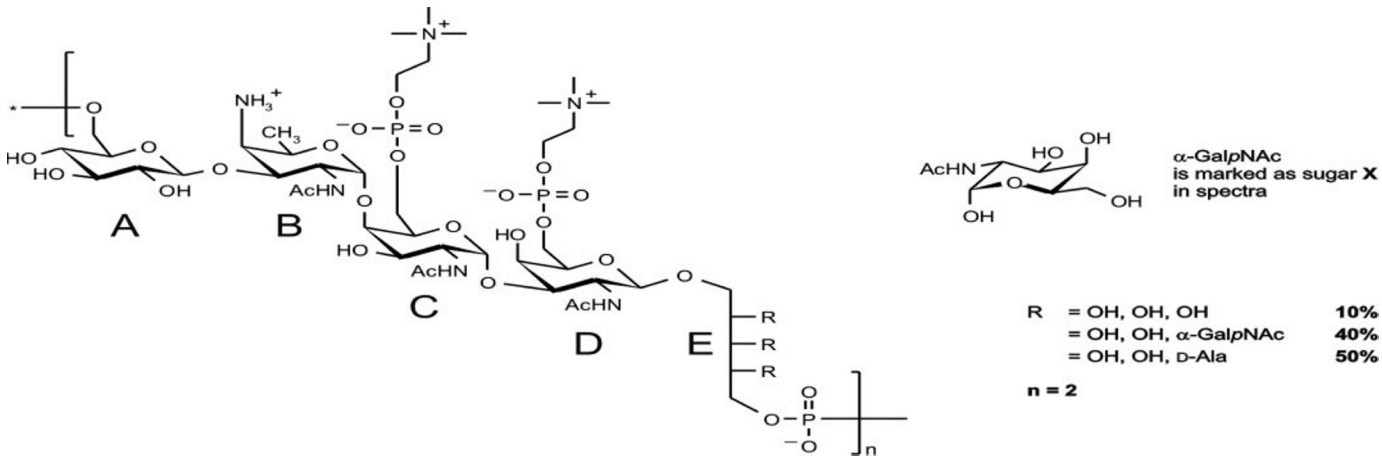

FIGURE 12. **Structure and substitution pattern of the repeating unit of LTA isolated from *S. pneumoniae* strain Fp23.** The percentage of alanylation, glycosylation, and the average number of the repeating units were determined from the ^{1}H NMR spectrum.

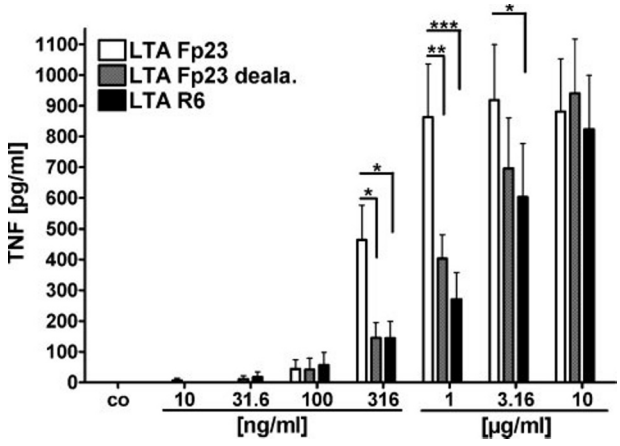

FIGURE 13. **Comparison of cytokine induction by LTA from *S. pneumoniae* R6, Fp23, and dealanylated LTA Fp23.** Human whole blood from eight healthy volunteers was stimulated with the given concentrations of either LTA for 22 h. TNF release was measured in the cell-free supernatants by ELISA. Data are means ± S.E. *, $p < 0.05$; **, $p < 0.01$; and ***, $p < 0.001$ (repeated-measure analysis of variance with Bonferroni multiple comparison test).

to have a low biological potency (13, 40, 41), whereas all of them used the chloroform-methanol extraction for the LTA isolation, which is more harsh than the butanol extraction and all examined *S. pneumoniae* strain R6 or the closely related R36A, but not LTA from Fp23.

These results indicated that the differences in the immunostimulatory potency of LTA Fp23 and LTA R6 must stem from differences in their chemical structure. We could confirm the published structure for the LTA R6 (11, 12), but two differences were observed. The LTA backbone only consisted of two repeating units instead of five to seven, resulting in a lower molecular mass of ~4 kDa, and an additional *N*-acetyl-D-galactosamine was found at the ribitol. Interestingly, the LTA Fp23 additionally carried bound D-alanine at the ribitol. This represents a new type of microheterogeneity in addition to the differences in the chain length of the LTA backbone, the fatty acids, and the substitution, because here for the first time a heterogeneity in the position of the substituent on different hydroxyl groups is described. In comparison, in LTAs from *S. aureus* glycerol is present instead of the ribitol, and therefore alanylation can only occur at a single fixed position. However, in the pneumococcal LTA the D-alanine is equally distributed over all three secondary hydroxyls of the ribitol. Despite the constant hydrolysis of the alanine esters, a high D-alanine content is observed in the isolated material, which makes it highly probable that the LTA is synthesized as a fully alanylated product.

As the D-alanine determines the potency of staphylococcal LTA, and because this was the only structural difference observed between the two pneumococcal LTAs, this could explain the greater potency of LTA Fp23 to induce cytokine release. This was confirmed by dealanylation of LTA Fp23, which resulted in a reduction of cytokine-inducing potency of LTA Fp23 to that of LTA R6. These observations correspond with the results from Brueckner *et al.*,[4] who report that the *dltA* gene of *S. pneumoniae* R6 showed a mutation resulting in a stop codon so that the *dltA* and *dltB* genes are knocked out. This should lead to an inability to alanylate LTA. So, the D-alanine content of the LTA from *S. pneumoniae* seems to be crucial for full immunostimulatory potency as shown also for staphylococcal LTA (19). In that study, several synthetic LTAs with small differences in their molecular structures were used to determine which LTA substituent is necessary for the immunostimulatory potency of LTA. Synthetic LTA is a useful tool, especially because isolated native LTA are characterized by microheterogeneity, *e.g.* the variability of substituents on the hydroxyl groups of the ribitol moiety in the pneumococcal LTA. A synthetic pneumococcal LTA would help to elucidate the core structure of the pneumococcal LTA that is necessary to activate immune cells. We also aim to clarify the interaction between LTA and the receptors, especially with regard to the role of D-alanine in receptor binding.

Taken together, the presence of D-alanine substituents, shown here for the first time in pneumococcal LTA from the strain Fp23, confers full immunostimulatory potency comparable to that of LTA from *S. aureus*, whereas the presence of the more complex pentamer repeating unit instead of polyglycerol in the backbone and the shorter backbone length do not affect the immunostimulatory potency of the LTA. Previous findings of weaker immunostimulatory activity of *S. pneumoniae* LTA

[4] M. Kovacs, A. Halfmann, I. Fedtke, M. Heintz, A. Peschel, W. Vollmer, R. Hakenbeck, and R. Brückner, personal communication, manuscript submitted.

appear to be linked to the choice of a laboratory strain, which lacks D-alanylation and pathogenicity. Whether the latter characteristics are linked represents an interesting hypothesis.

Acknowledgments—We are grateful for the prompt help by Philippa Mang and for the excellent technical assistance by Leonardo Cobianchi, Silvia Asmus, and Margarete Kreuer-Ullmann.

REFERENCES

1. Organization, W. H. (1998) *Wkly. Epidemiol. Rec.* **73,** 187–188
2. Zangwill, K. M., Vadheim, C. M., Vannier, A. M., Hemenway, L. S., Greenberg, D. P., and Ward, J. I. (1996) *J. Infect. Dis.* **174,** 752–759
3. Stool, S. E., and Field, M. J. (1989) *Pediatr. Infect. Dis. J.* **8,** S11–S14
4. Jedrzejas, M. J. (2001) *Microbiol. Mol. Biol. Rev.* **65,** 187–207; first page, table of contents
5. Henrichsen, J. (1995) *J. Clin. Microbiol.* **33,** 2759–2762
6. Trollfors, B., Burman, L., Dannetun, E., Llompart, J., and Norrby, R. (1983) *J. Clin. Microbiol.* **18,** 978–980
7. Farrell, D. J., Jenkins, S. G., and Reinert, R. R. (2004) *J. Med. Microbiol.* **53,** 1109–1117
8. Bridy-Pappas, A. E., Margolis, M. B., Center, K. J., and Isaacman, D. J. (2005) *Pharmacotherapy* **25,** 1193–1212
9. Novak, R., Henriques, B., Charpentier, E., Normark, S., and Tuomanen, E. (1999) *Nature* **399,** 590–593
10. Canton, R., Morosini, M., Enright, M. C., and Morrissey, I. (2003) *J. Antimicrob. Chemother.* **52,** 944–952
11. Fischer, W. (1997) *Microb. Drug Resist* **3,** 309–325
12. Behr, T., Fischer, W., Peter-Katalinic, J., and Egge, H. (1992) *Eur. J. Biochem.* **207,** 1063–1075
13. Han, S. H., Kim, J. H., Martin, M., Michalek, S. M., and Nahm, M. H. (2003) *Infect. Immun.* **71,** 5541–5548
14. Schroder, N. W., Morath, S., Alexander, C., Hamann, L., Hartung, T., Zahringer, U., Gobel, U. B., Weber, J. R., and Schumann, R. R. (2003) *J. Biol. Chem.* **278,** 15587–15594
15. Briles, E. B., and Tomasz, A. (1973) *J. Biol. Chem.* **248,** 6394–6397
16. Briese, T., and Hakenbeck, R. (1985) *Eur. J. Biochem.* **146,** 417–427
17. Morath, S., Geyer, A., and Hartung, T. (2001) *J. Exp. Med.* **193,** 393–397
18. Morath, S., Geyer, A., Spreitzer, I., Hermann, C., and Hartung, T. (2002) *Infect. Immun.* **70,** 938–944
19. Deininger, S., Stadelmaier, A., von Aulock, S., Morath, S., Schmidt, R. R., and Hartung, T. (2003) *J. Immunol.* **170,** 4134–4138
20. Henneke, P., Morath, S., Uematsu, S., Weichert, S., Pfitzenmaier, M., Takeuchi, O., Muller, A., Poyart, C., Akira, S., Berner, R., Teti, G., Geyer, A., Hartung, T., Trieu-Cuot, P., Kasper, D. L., and Golenbock, D. T. (2005) *J. Immunol.* **174,** 6449–6455
21. Grangette, C., Nutten, S., Palumbo, E., Morath, S., Hermann, C., Dewulf, J., Pot, B., Hartung, T., Hols, P., and Mercenier, A. (2005) *Proc. Natl. Acad. Sci. U. S. A.* **102,** 10321–10326
22. Tettelin, H., Nelson, K. E., Paulsen, I. T., Eisen, J. A., Read, T. D., Peterson, S., Heidelberg, J., DeBoy, R. T., Haft, D. H., Dodson, R. J., Durkin, A. S., Gwinn, M., Kolonay, J. F., Nelson, W. C., Peterson, J. D., Umayam, L. A., White, O., Salzberg, S. L., Lewis, M. R., Radune, D., Holtzapple, E., Khouri, H., Wolf, A. M., Utterback, T. R., Hansen, C. L., McDonald, L. A., Feldblyum, T. V., Angiuoli, S., Dickinson, T., Hickey, E. K., Holt, I. E., Loftus, B. J., Yang, F., Smith, H. O., Venter, J. C., Dougherty, B. A., Morrison, D. A., Hollingshead, S. K., and Fraser, C. M. (2001) *Science* **293,** 498–506
23. Hartung, T., and Wendel, A. (1995) *Altex* **12,** 70–75
24. von Aulock, S., Morath, S., Hareng, L., Knapp, S., van Kessel, K. P., van Strijp, J. A., and Hartung, T. (2003) *Immunobiology* **208,** 413–422
25. Kellogg, T. A., Lazaron, V., Wasiluk, K. R., and Dunn, D. L. (2001) *Shock* **15,** 124–129
26. Klein, R. A., Hartmann, R., Egge, H., Behr, T., and Fischer, W. (1994) *Carbohydr. Res.* **256,** 189–222
27. Klein, R. A., Hartmann, R., Egge, H., Behr, T., and Fischer, W. (1996) *Carbohydr. Res.* **281,** 79–98
28. Fischer, W., Behr, T., Hartmann, R., Peter-Katalinic, J., and Egge, H. (1993) *Eur. J. Biochem.* **215,** 851–857
29. Karlsson, C., Jansson, P. E., and Skov Sorensen, U. B. (1999) *Eur. J. Biochem.* **265,** 1091–1097
30. Karlsson, C., Jansson, P. E., and Sorensen, U. B. (1998) *Eur. J. Biochem.* **255,** 296–302
31. Bergstrom, N., Jansson, P. E., Kilian, M., and Skov Sorensen, U. B. (2000) *Eur. J. Biochem.* **267,** 7147–7157
32. Vialle, S., Sepulcri, P., Dubayle, J., and Talaga, P. (2005) *Carbohydr. Res.* **340,** 91–96
33. Shabarova, Z. A., Hughes, N. A., and Baddiley, J. (1962) *Biochem. J.* **83,** 216–219
34. Neuhaus, F. C., and Baddiley, J. (2003) *Microbiol. Mol. Biol. Rev.* **67,** 686–723
35. AlonsoDeVelasco, E., Verheul, A. F., Verhoef, J., and Snippe, H. (1995) *Microbiol. Rev.* **59,** 591–603
36. Schneider, O., Michel, U., Zysk, G., Dubuis, O., and Nau, R. (1999) *Neurology* **53,** 1584–1587
37. Stuertz, K., Schmidt, H., Eiffert, H., Schwartz, P., Mader, M., and Nau, R. (1998) *Antimicrob. Agents Chemother.* **42,** 277–281
38. Triantafilou, M., Manukyan, M., Mackie, A., Morath, S., Hartung, T., Heine, H., and Triantafilou, K. (2004) *J. Biol. Chem.* **279,** 40882–40889
39. Echchannaoui, H., Frei, K., Schnell, C., Leib, S. L., Zimmerli, W., and Landmann, R. (2002) *J. Infect. Dis.* **186,** 798–806
40. Bhakdi, S., Klonisch, T., Nuber, P., and Fischer, W. (1991) *Infect. Immun.* **59,** 4614–4620
41. Kim, J. H., Seo, H., Han, S. H., Lin, J., Park, M. K., Sorensen, U. B., and Nahm, M. H. (2005) *Infect. Immun.* **73,** 834–840